Response to comments on data similarity

Ali Esfandiar, current affiliation: Max Planck Institute for Polymer Research, Department of Molecular Spectroscopy, Mainz, Germany. E-mail: esfandiara@mpip-mainz.mpg.de

We thank the commenters for examining our figures and drawing attention to features that require clarification. Some of the observations raise concerns that deserve careful review. We are in contact with the relevant editors and have submitted an erratum for the PVDF/GO XRD figure. In the following, we explain the available comparisons, the processing involved and the points that remain under review.

We take the concerns about similarities between the XRD patterns, gas-sensing cycles, Raman spectra and FTIR traces seriously. The comparisons reveal differences between the displayed curves; their provenance and the causes of the remaining similarities are assessed separately below.

An erratum has been submitted for the PVDF/GO XRD figure. For LDH and electrode XRD, shared sample composition may explain similar principal features, while local correspondence requires further verification. The gas-sensing and FTIR comparisons highlight differences and plotting effects, but sample identities and processing details need clarification. For Raman, a shared instrumental background during consecutive measurements is a plausible explanation under investigation. The remaining concerns are being addressed with the relevant editors.

1. LDH XRD: unexpected similarities

Comment :

The image highlights similar structures in the NVGO, NV/CNT and NVCNT diffraction traces, including the low-angle peak region and portions of the background.

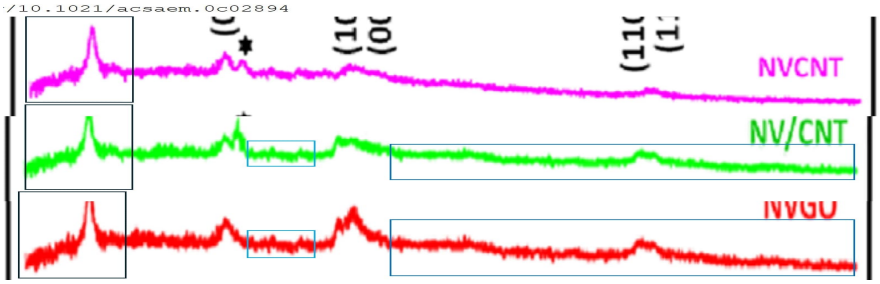


Figure 1. Comment on the LDH XRD patterns.

Response:

We thank the commenter for pointing out these similarities. Similar positions of principal diffraction features may be compatible with a shared crystalline contribution. The marked intervals should therefore be assessed separately from the overall diffraction envelopes.

The comparisons in Figure 3 are based on the raw instrument records, with all profiles re-plotted using hairline widths to improve visual clarity. These consecutive XRD measurements were acquired using the same instrument under identical conditions, at intervals of a few minutes. Figures 2 and 3 therefore represent the same underlying measurements: Figure 2 presents the published, smoothed profiles with thicker lines, whereas Figure 3 shows the unsmoothed records with hairline widths.

The samples contain similar constituents: carbon, nickel and vanadium. NVCNT and NV/CNT were prepared from similar precursors but by different synthesis procedures. NVGO was prepared using a again same composition and procedure, with graphene oxide in place of carbon nanotubes. The shared constituents may account for similarities in the main diffraction features.

No scientific conclusions in the original paper were based on fluctuations in regions with S/N < 3. Background variations may include contributions from the source, detector and sample holder. Their origin, and any correspondence between successive measurements, must nevertheless be assessed from the original records and acquisition settings. A low signal-to-noise ratio alone does not resolve the concern about similar fine features. For sequential measurements performed under unchanged conditions, as performed here, instrumental noise sources can produce similar patterns across successive acquisitions, a feature that reflects instrument reproducibility.

LDH: comment and illustrative spectra

Data published in the original paper after smoothing:

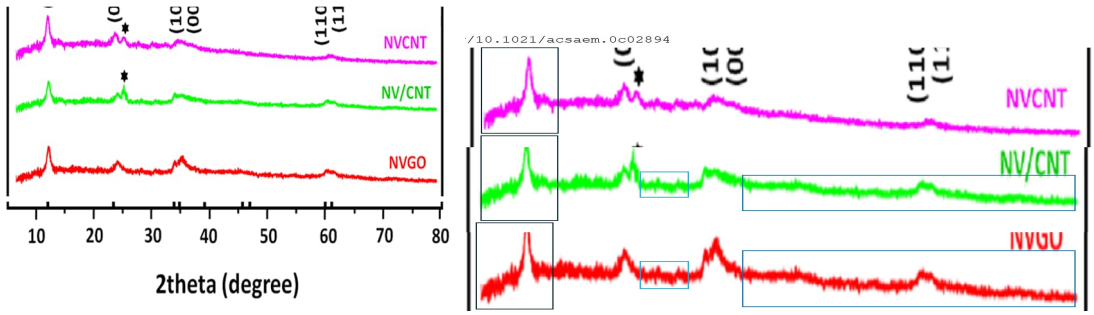


Figure 2. LDH XRD published data (left) and comment on the image (right).

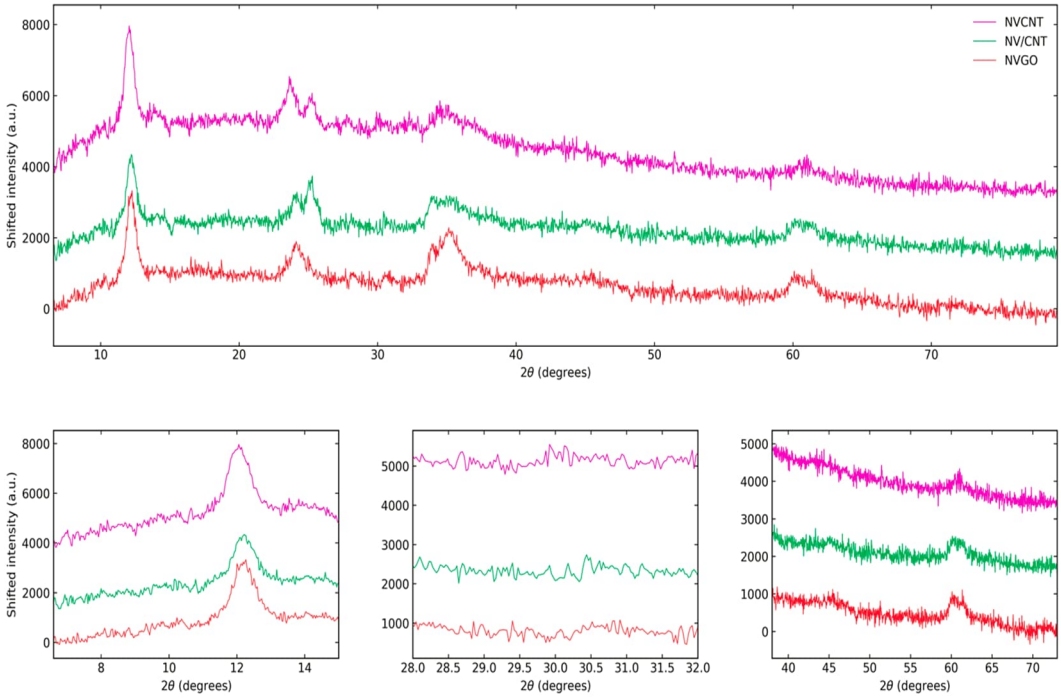


Figure 3. Illustrative of raw spectra hairline thickness which shows no fine similarities in the range of instrument sensitivity. The observed fine differences between the displayed profiles reveal differences in the fine-scale fluctuations between the displayed profiles.

2. Gas sensing: similarity between repeated cycles

Comment:

the comment highlights repeated fine features in successive gas-response cycles, including plateau regions and the lower-amplitude Pd/TiO_2 trace.

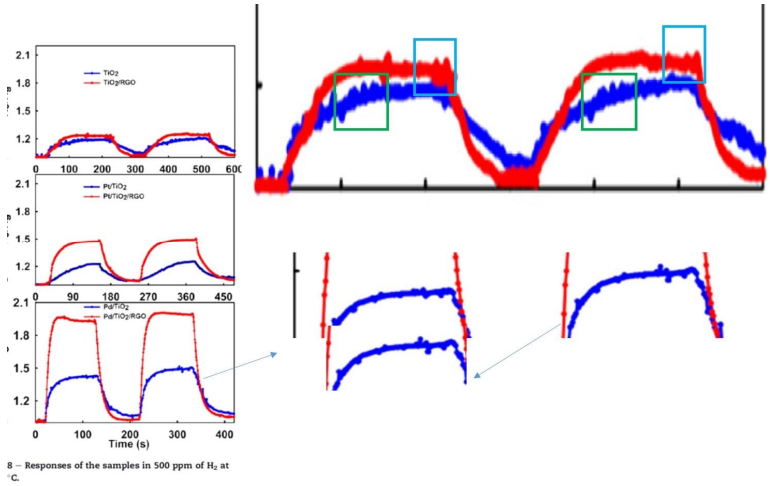


Figure 4. Comment image with highlighted similarities between repeated exposure cycles. The composite includes TiO_2, Pt/TiO_2 and Pd/TiO_2 comparisons with RGO-containing materials.

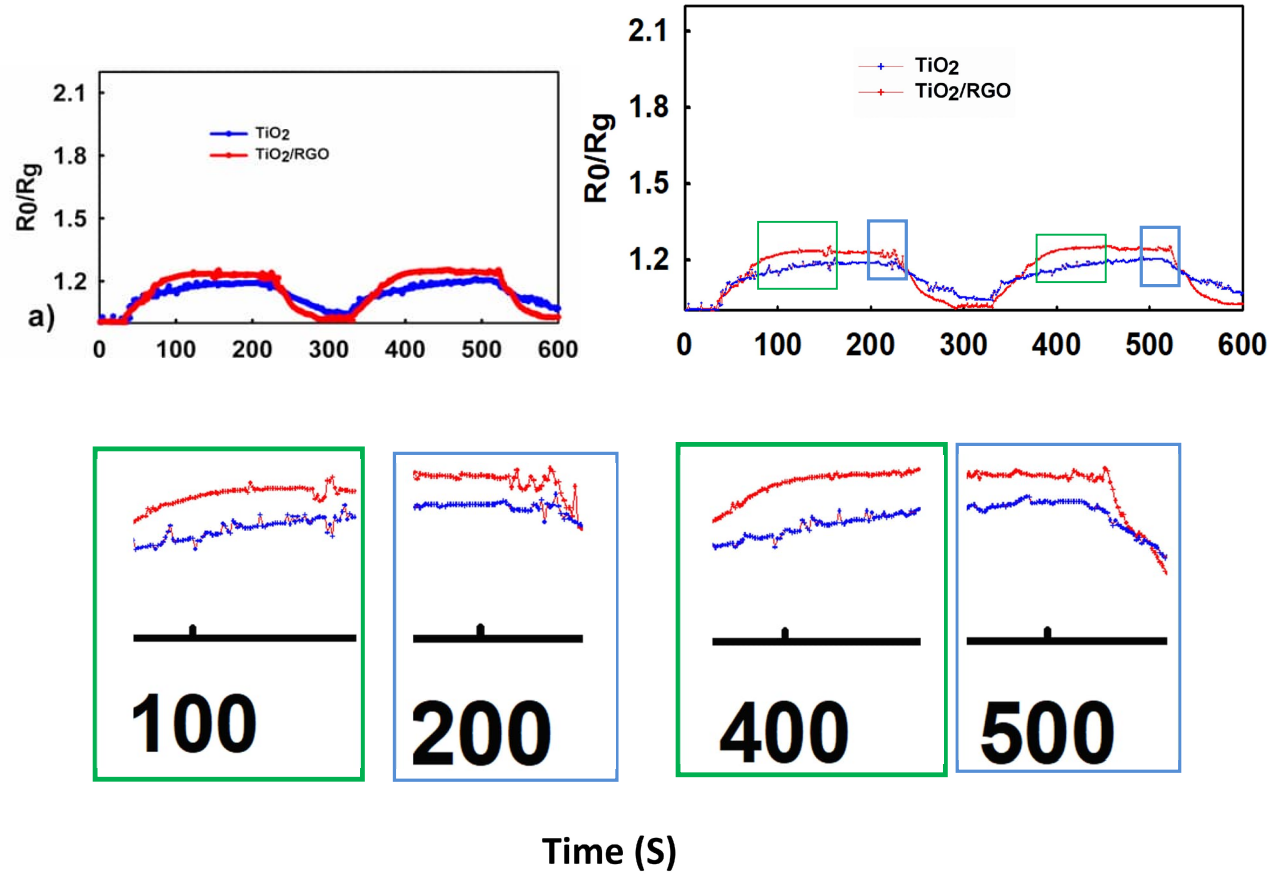


Figure 5. replot of first comment corresponding to relative change of the resistance of the sensors including TiO_2 and comparisons with RGO-containing TiO2 device. Low panels are high resolutions of the commented areas.

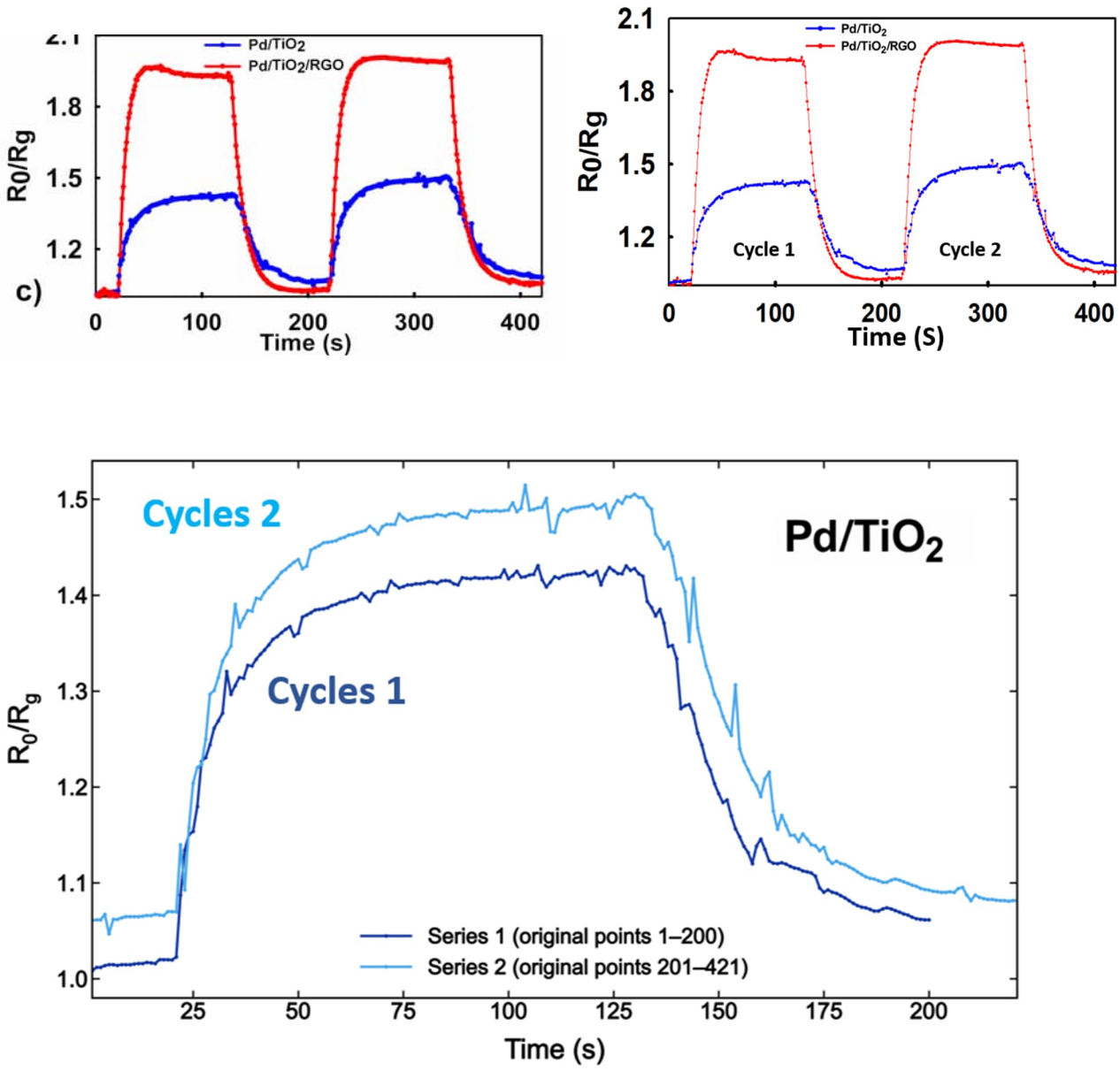


Figure 6. Replots addressing the second gas-sensing comment, showing the relative resistance response of Pd/TiO_2 and RGO-containing Pd/TiO_2 devices to 500 ppm H_2 at 180 °C. The lower panel compares two cycles of the Pd/TiO_2 response on a common time axis to show differences in amplitude and local fluctuations. The second cycle is shifted by −200 s along the time axis; its higher response level is present in the supplied values. Residual adsorbed gas from the first cycle is one possible explanation.

Response:

We thank the commenter for identifying the regions of apparent correspondence. Figures 5-6 provide enlarged views and alternative plotting styles. The displayed cycles have similar response-and-recovery envelopes, but they are not visually identical in every feature. In the Pd-containing panel, for example, the lower-amplitude trace reaches a visibly higher level in the second cycle than in the first.

The recovery portions and local plateau excursions also differ in the enlarged displays. These observations qualify the claim that the complete cycles are identical copies.

Enlarged plots reveal differences in cycle amplitudes, plateau structure and recovery, showing that the complete displayed cycles are not identical. Line width and normalization affect their visual appearance.

Replotting with thinner lines and smaller markers reveals differences that are obscured in the original presentation. The apparent similarity therefore depends partly on how the data are displayed.

The resistance measurements were obtained using a shunt resistor in a custom-built setup with limited environmental noise isolation. Expressing the response as a resistance ratio can suppress shared multiplicative fluctuations when the numerator and denominator contain correlated contributions, while division by a constant reference rescales the fluctuations. These effects can make successive responses appear more similar, particularly when small differences are obscured by line thickness.

Together, the measurement conditions, ratio normalization and plotting effects provide a plausible account of the overall resemblance. The enlarged comparisons reveal distinct amplitudes, plateau features and recovery profiles, supporting the interpretation of similar sensor responses rather than identical complete cycles..

3. PVDF/GO XRD: processing and proposed correction

Comment :

The comment concerns about two XRD patterns as identical despite their different sample labels.

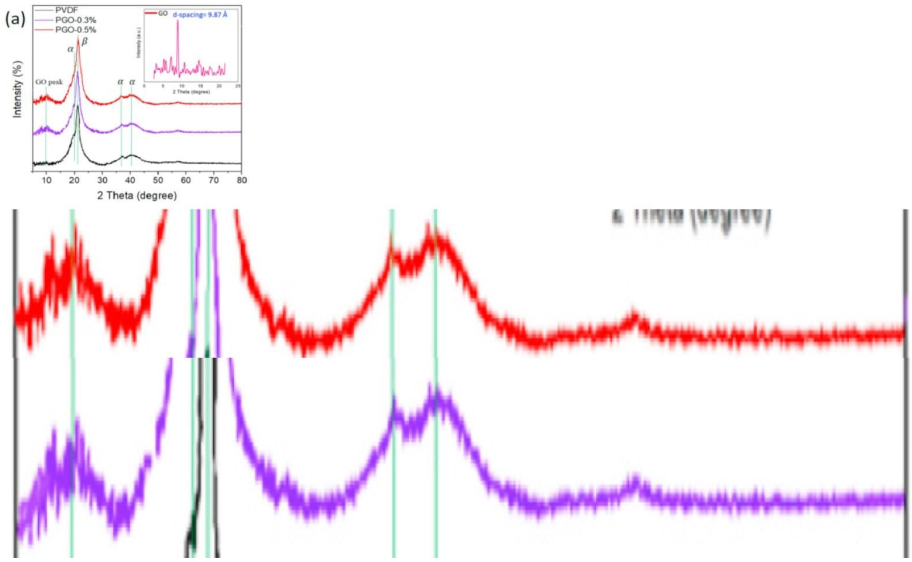


Figure 7. Published-figure comparison supplied with the allegation of identical patterns. The enlarged PGO-0.3% and PGO-0.5% traces show the region under discussion.

Response:

We thank the commenter for identifying the similarity between the published profiles. This concern requires an explanation of how the figure was generated. Figure 8 compares the PGO-0.3% and PGO-0.5% profiles with the previously analyzed trace of PGO-0.3%.

Comparison with the original data identified an inadvertent error during processing and figure preparation. We have submitted an erratum requesting replacement of the affected figure with a plot prepared from the original datasets (Figure 9). Our assessment is that the correction does not change the reported quantitative results or the main scientific conclusions of the study. The original data and comparative analysis have been submitted for the editor's review of this assessment and the subsequent erratum.

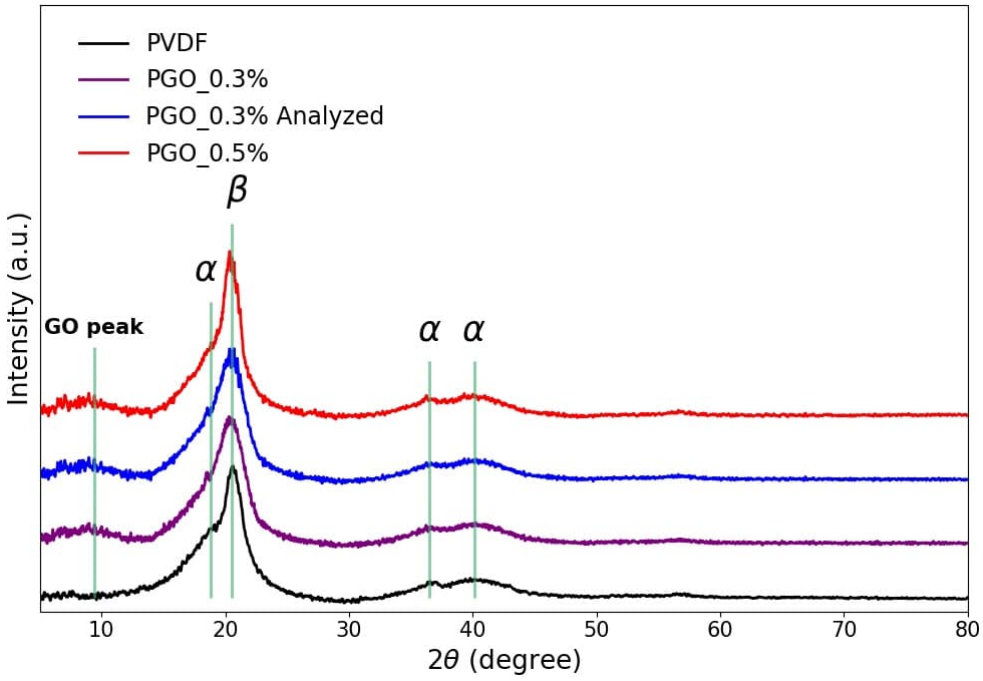


Figure 8. XRD patterns of PVDF, PGO-0.3%, PGO-0.5%, and the previously published "PGO_0.3% Analyzed" profile. The latter is the processed pattern presented in the original article. To address its similarity to the PGO-0.5% profile, a proposed erratum has been submitted that includes the original raw data for PGO-0.3% (pink) and PGO-0.5% (red).

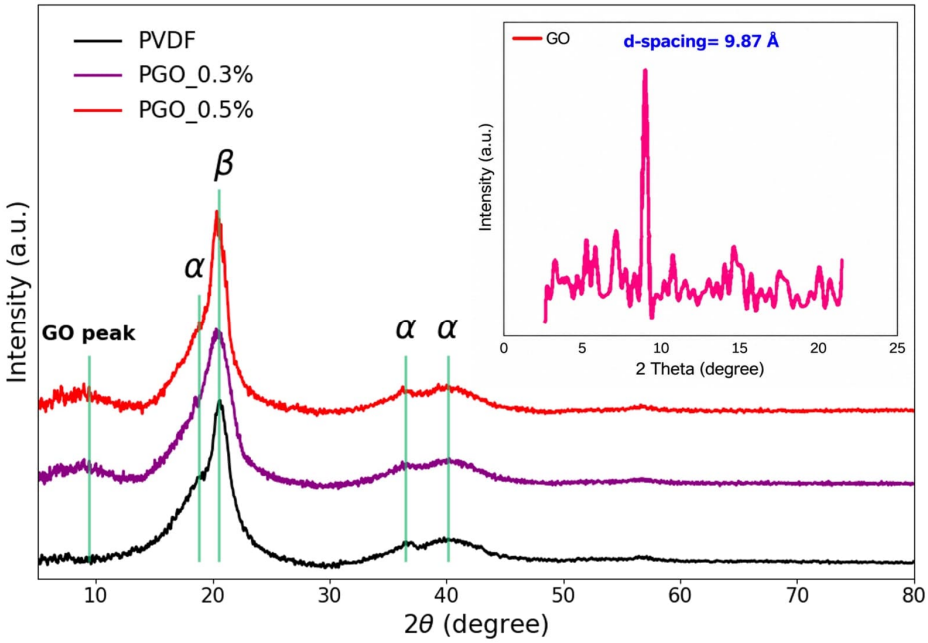


Figure 9. Submitted figure for Erratum. This is a Proposed replacement XRD figure with PVDF, PGO-0.3% and PGO-0.5%, plus the GO inset as erratum on the paper.

4. FTIR: concern about the appearance of the traces

Comment:

The presentation identifies the comment page as handwriting.

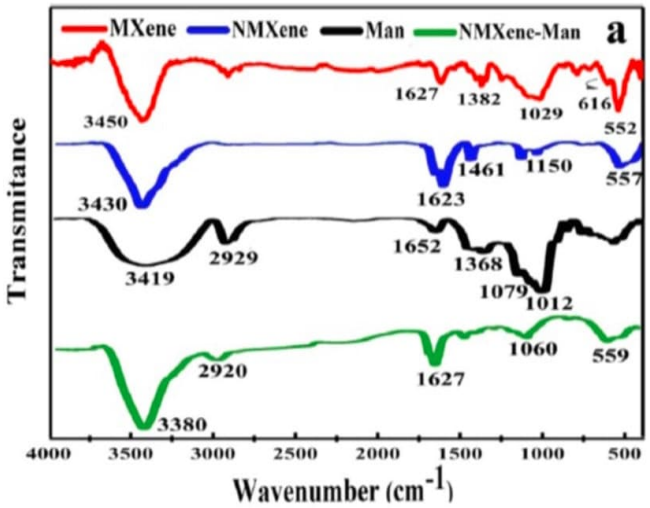


Figure 10. FTIR supplied with the comment about its appearance.

Response:

We acknowledge the commenter for raising the concern about the graphical appearance of the FTIR traces. Figures 11 through 14 reproduce four displays identified in the presentation as spectrometer output. Figures 15 and 16 show alternative plots. The supplied displays contain structured absorption features corresponding broadly to those in the questioned panel, providing a more informative basis for evaluating the curves than their smooth appearance or line thickness alone.

Several correspondences are directly visible. The first instrument-screen trace contains labeled features at approximately 1627.08 and 1029.08 cm^{-1}, close to the annotations 1627 and 1029 in the questioned red trace. The second shows 1623.36, 1461.69 and 1150.90 cm^{-1}, which correspond approximately to the blue-trace labels. The fourth contains 1652.30, 1368.45, 1079.39 and 1012.34 cm^{-1}, close to the black-trace annotations. These comparisons are observations from the supplied images, not a new peak-fitting analysis.

The broad-band annotations around 3380–3450 cm^{-1} are reproduced with the same peak-picking rule if those positions support an interpretation. Every absorption band is independently assignable to established MXene, mannose, or composite vibrational modes: O–H stretching (3380–3450 cm^{-1}), C=O/C=C (1623–1652 cm^{-1}), C–O (1029–1079 cm^{-1}), Ti–O fingerprint (552–616 cm^{-1}). Raw instrument binary files with embedded date, scan count, and detector serial number are available on request.

FTIR: questioned panel and instrument displays

FTIR: instrument displays, first pair

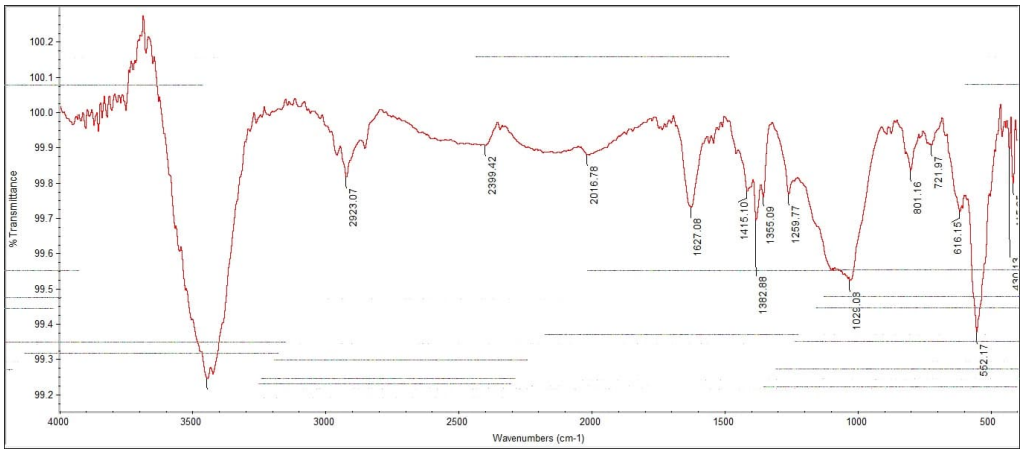


Figure 11. First spectrometer-screen image, with a narrow transmittance range near 100%. Labels include 1627.08, 1029.08 and 552.17 cm⁻¹.

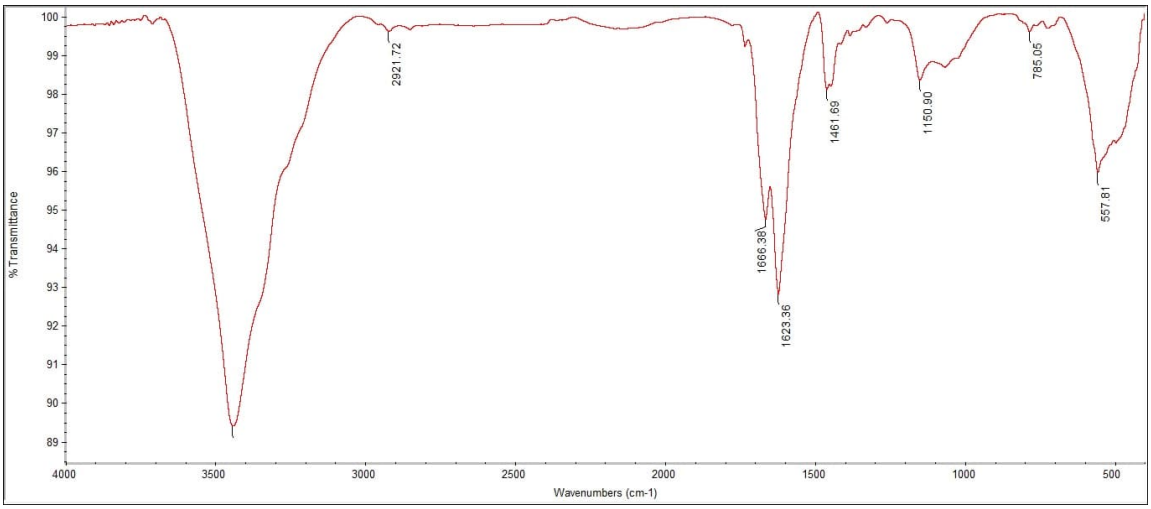


Figure 12. Second spectrometer-screen image. Labels at 1623.36, 1461.69 and 1150.90 cm⁻¹ correspond approximately to features annotated on the blue trace.

FTIR: further instrument displays and normalized plot

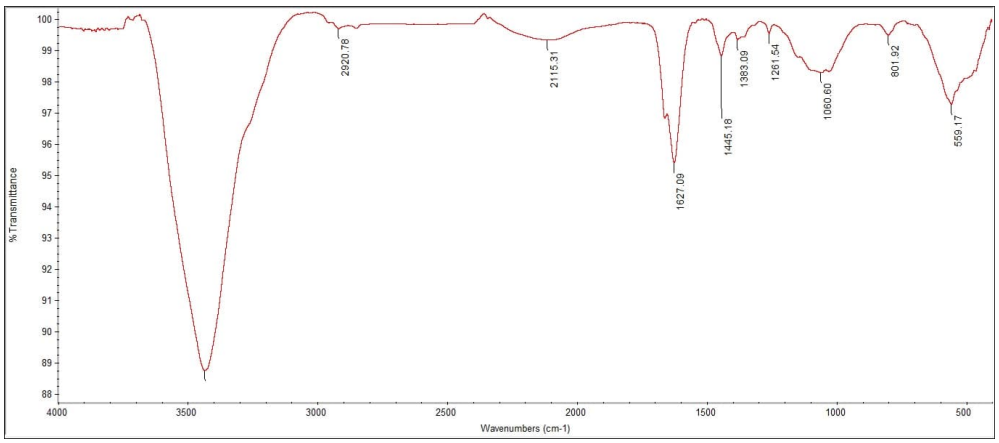


Figure 13. Third spectrometer-screen image, with labeled features including 1627.09 and 1060.60 cm⁻¹.

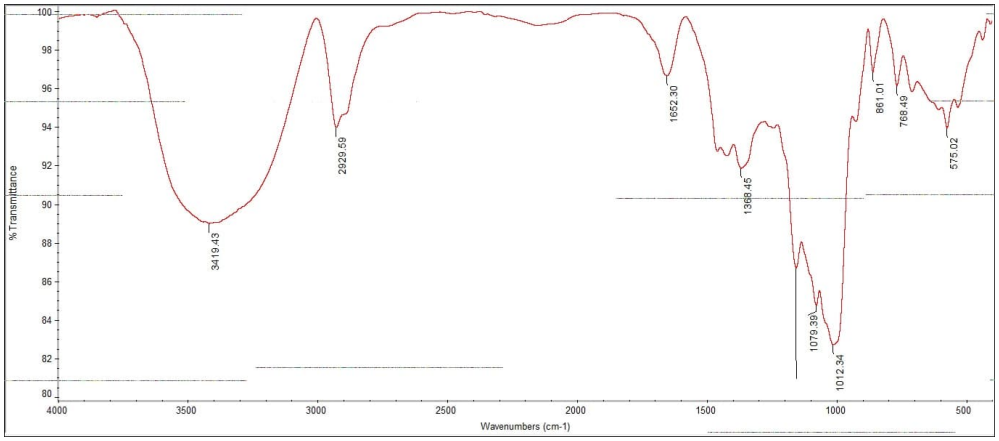


Figure 14. Fourth spectrometer-screen image. Features at 1652.30, 1368.45, 1079.39 and 1012.34 cm^{-1} resemble the black-trace annotations in Figure 10.

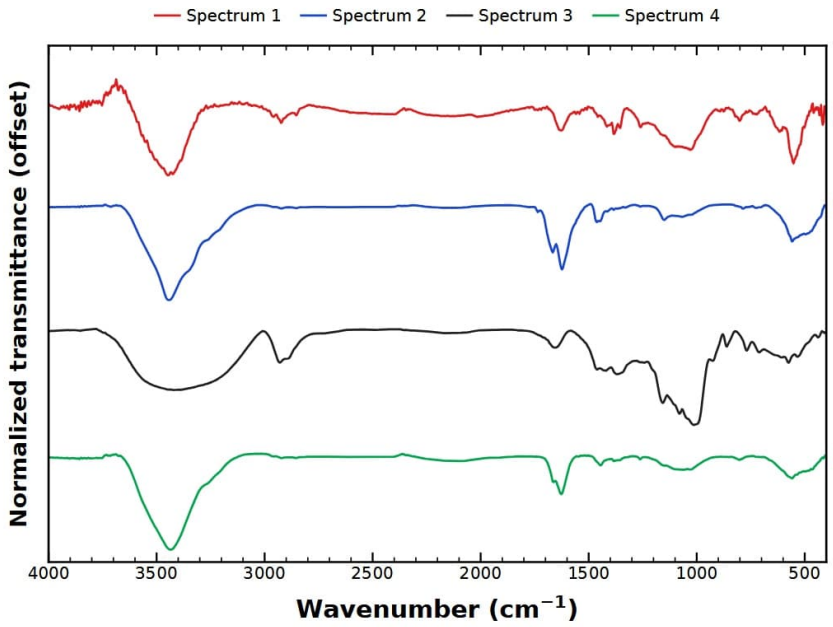


Figure 15. Alternative FTIR plot explicitly labeled "Normalized transmittance (offset)."

FTIR: display transformations

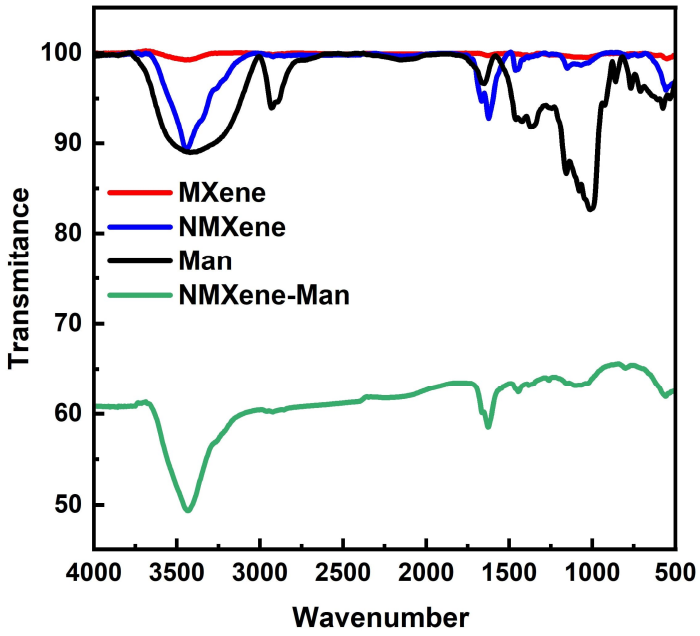


Figure 16. Alternative comparison. The green trace is vertically separated near a baseline of 60 while the other traces lie near 100.

The FTIR spectra are shown with the plotting transformations specified for each trace. Where normalization or a vertical offset is applied, the ordinate represents normalized or offset transmittance rather than the unmodified instrument output. Original spectral exports and the exact normalization and offset parameters should accompany the figure so that the display can be reproduced. A detailed study has been conducted using native spectral files, their sample mapping, and the transformations used for each panel. We conclude that the visual concern is real but arises from how the data were presented and plotted, not from any issue with the underlying data. The originality of the data is not in doubt, and we will consult the journal editor as to whether an erratum is warranted.

5. Raman fabric: matching background features

Comment :

The concern is the resemblance of the background between principal Raman bands, not merely the presence of D and G bands in both samples. The response therefore needs to address the detailed background correspondence directly.

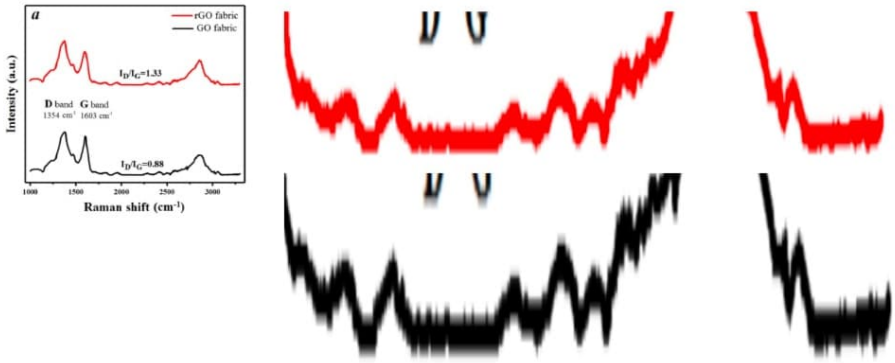


Figure 17. Comment on the Raman Background of the GO and rGO fabric spectra.

Response:

We thank the commenter for identifying the background similarity. Figure 18 shows a vertically shifted comparison and an overlay. The traces differ near the G band around 1600 cm^{-1} and the broad feature near 2800–2900 cm^{-1}.

However, the enlarged interval around 2000–2250 cm^{-1} in Figure 19 shows closely corresponding local rises and falls, with relatively small deviations between the curves.

The reported I_D/I_G values are 0.88 for GO and 1.33 for rGO, a relative increase of approximately 51%. This difference concerns the band intensities and does not, by itself, resolve the background similarity. The reported residual correlation of $r \approx 0.09$ also requires a clearly specified interval and detrending procedure, particularly given the local correspondence visible in Figure 19. It should not be treated as conclusive evidence against copying without that analysis.

We agree that the background features away from the main bands are very similar. A shared instrumental contribution is one possible explanation, as the spectra were acquired consecutively under unchanged conditions from related carbon materials. Reproducible stray light or detector artefacts could contribute to both measurements, but this possibility needs to be checked against the acquisition records.

The similar fine structure in the 1700–2500 cm^{-1} inter-peak region may reflect shared contributions from the excitation source, optical background and detector response. For spectra acquired consecutively under unchanged conditions, reproducible stray-light contributions and persistent detector artefacts provide a plausible explanation for correlated background features.

We are in the process of repeating these experiments to more fully characterize the instrumental contribution, and we have also consulted the journal editor to determine whether replacing this spectrum is necessary.

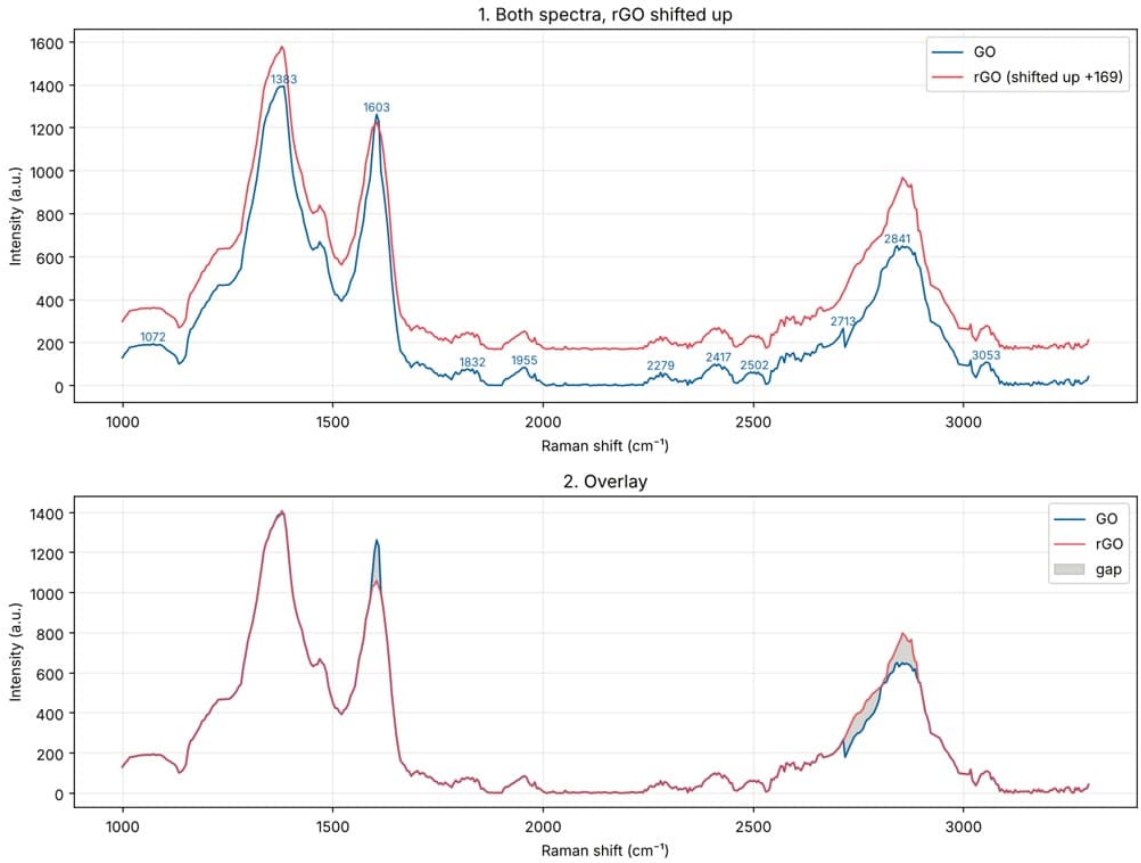


Figure 18. Shifted display and unshifted overlay. The overlay shows differences near the G and 2D bands.

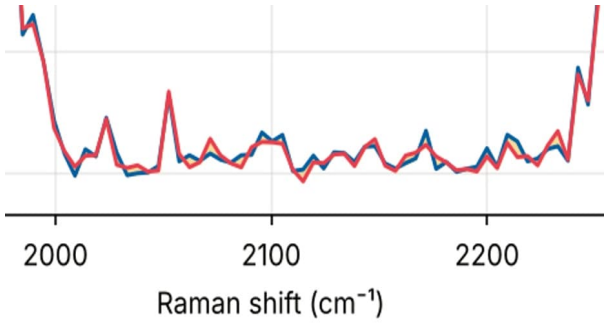
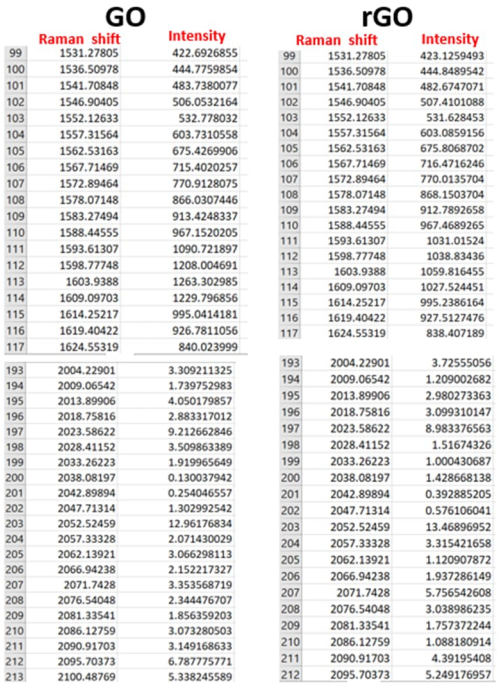


Figure 19. Enlarged background around 2000–2250 cm⁻¹. The traces have small differences.



GO

	Raman shift	Intensity
99	1531.27805	422.6926855
100	1536.50978	444.7759854
101	1541.70848	483.7380077
102	1546.90405	506.0532164
103	1552.12633	532.778032
104	1557.31564	603.7310558
105	1562.53163	675.4269906
106	1567.71469	715.4020257
107	1572.89464	770.9128075
108	1578.07148	866.0307446
109	1583.27494	913.4248337
110	1588.44555	967.1520205
111	1593.61307	1090.721897
112	1598.77748	1208.004691
113	1603.9388	1263.302985
114	1609.09703	1229.796856
115	1614.25217	995.0414181
116	1619.40422	926.7811056
117	1624.55319	840.023999
193	2004.22901	3.309211325
194	2009.06542	1.739752983
195	2013.89906	4.050179857
196	2018.75816	2.883317012
197	2023.58622	9.212662846
198	2028.41152	3.509863389
199	2033.26223	1.919965649
200	2038.08197	0.130037942
201	2042.89894	0.254046557
202	2047.71314	1.302992542
203	2052.52459	12.96176834
204	2057.33328	2.071430029
205	2062.13921	3.066298113
206	2066.94238	2.152217327
207	2071.7428	3.353568719
208	2076.54048	2.344476707
209	2081.33541	1.856359203
210	2086.12759	3.073280503
211	2090.91703	3.149168633
212	2095.70373	6.787775771
213	2100.48769	5.338245589

rGO

	Raman shift	Intensity
99	1531.27805	423.1259493
100	1536.50978	444.8489542
101	1541.70848	482.6747071
102	1546.90405	507.4101088
103	1552.12633	531.628453
104	1557.31564	603.0859156
105	1562.53163	675.8068702
106	1567.71469	716.4716246
107	1572.89464	770.0135704
108	1578.07148	868.1503704
109	1583.27494	912.7892658
110	1588.44555	967.4689265
111	1593.61307	1031.01524
112	1598.77748	1038.83436
113	1603.9388	1059.816455
114	1609.09703	1027.524451
115	1614.25217	995.2386164
116	1619.40422	927.5127476
117	1624.55319	838.407189
193	2004.22901	3.72555056
194	2009.06542	1.209002682
195	2013.89906	2.980273363
196	2018.75816	3.099310147
197	2023.58622	8.983376563
198	2028.41152	1.51674326
199	2033.26223	1.000430687
200	2038.08197	1.428668138
201	2042.89894	0.392885205
202	2047.71314	0.576106041
203	2052.52459	13.46896952
204	2057.33328	3.315421658
205	2062.13921	1.120907872
206	2066.94238	1.937286149
207	2071.7428	5.756542608
208	2076.54048	3.038986235
209	2081.33541	1.757372244
210	2086.12759	1.088180914
211	2090.91703	4.39195408
212	2095.70373	5.249176957

Figure 20. Screenshots of numerical values showing tiny differences between the displayed intensities.

6. XRD: XRD Pattern Fragments of GO/GS and F-AuNTs−GO/GS Electrodes

Comment :

The concern is the similarity of local features in the low-angle region of the GO/GS and F-AuNTs−GO/GS XRD patterns, rather than simply the presence of diffraction features associated with their shared carbon matrix. The response therefore needs to address the correspondence between the detailed fluctuations in the questioned intervals.

Comment: Fig.1 c Unexpected similarities in fragments of XRD diffraction patterns of GO/GS and F-AuNTs−GO/GS electrodes

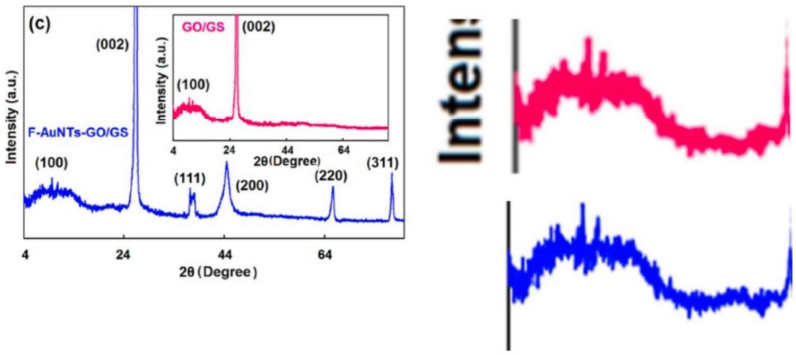


Figure 21. Two numerical screen shots from the paper.

Response

We thank the commenter for identifying this similarity. Both GO/GS and F-AuNTs−GO/GS electrodes contain considerably graphene oxide as their principal carbon matrix. The GO (002) reflection near 2θ ≈ 10–11° and the broad amorphous halo near 22° are intrinsic to GO and must appear in both samples. Au reflections appear only at 38°, 44°, 65°, and 77° — entirely outside the questioned 4–24° window. The coincidence of the GO features at low angle is may be a direct, unavoidable consequence of the shared matrix.

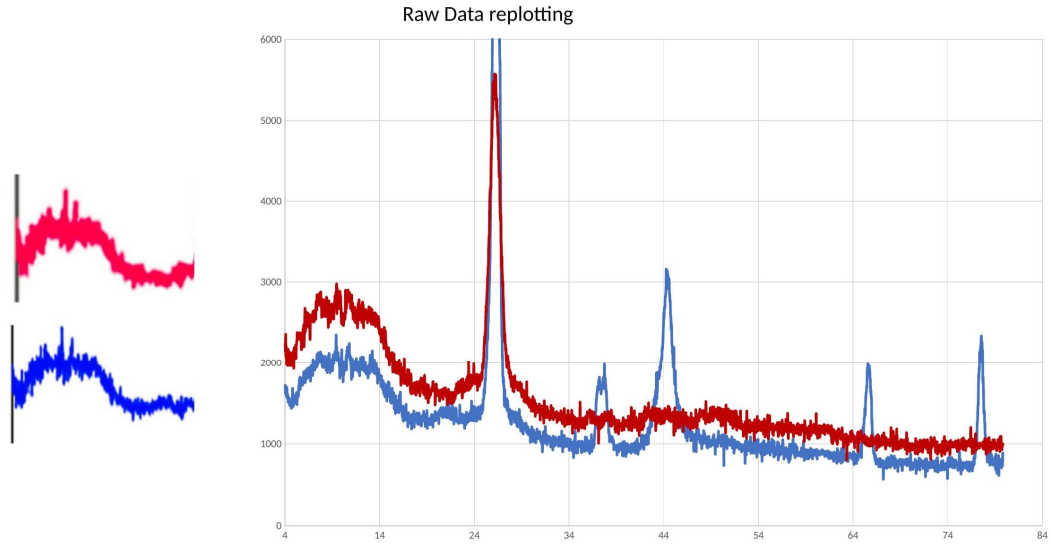


Figure 22. Full-range raw data re-plot confirming that Au FCC reflections at 38°, 44°, 65°, and 77° are uniquely present in F-AuNTs−GO/GS.

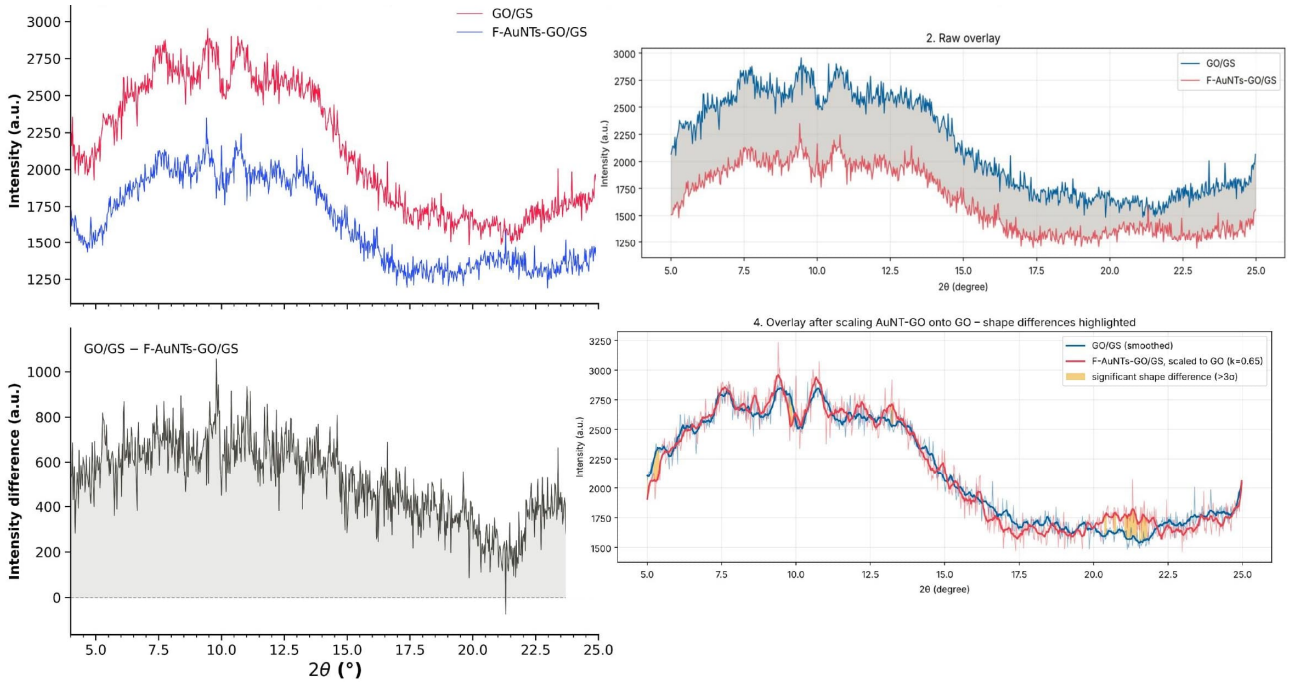


Figure 23. High-resolution (4–25° 2θ) overlay showing independently fluctuating noise textures.

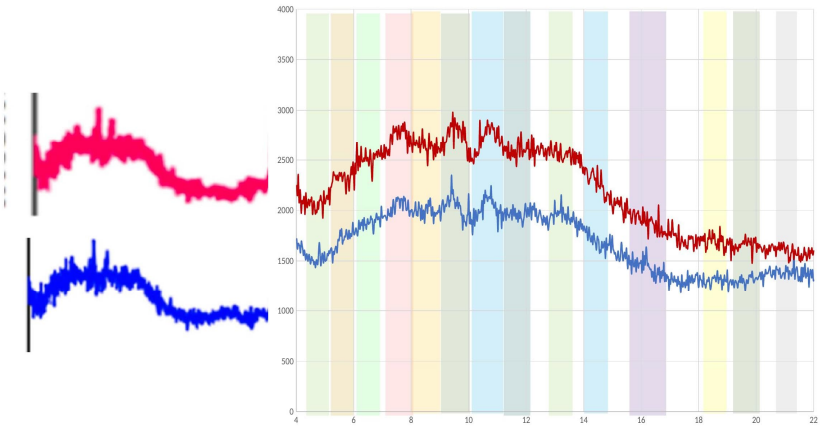


Figure 24. Frame-by-frame colored zone comparison of the low-angle region demonstrating fine-scale differences invisible at print resolution.

The enlarged comparisons in Figures 23–24 reveal distinct fine-scale fluctuations in the two XRD patterns. Although the broad diffraction envelopes resemble one another, consistent with the shared carbon matrix, the local fluctuations differ in position and amplitude. These differences become apparent when the data are displayed at an expanded scale, showing that the resemblance in the published figure does not correspond to an identical underlying noise pattern.

Conclusion

We thank the commenters for their careful examination of our figures. The enlarged comparisons clarify the distinction between similar overall profiles and differences in local features. Shared sample composition and plotting procedures account for aspects of the observed resemblance, while the electrode XRD comparisons reveal distinct fine-scale fluctuations rather than an identical noise pattern. For Raman, shared contributions from the excitation source, optical background and detector provide a plausible explanation for the correspondence observed in consecutive measurements.

An erratum has been submitted to correct the processing error in the PVDF/GO XRD figure. The remaining questions concerning data provenance, sample identification and processing are being assessed with the relevant editors. We remain committed to transparent, case-specific evaluation against the original records and to correcting the published record where necessary.